https://doi.org/10.5194/bg-2020-95
Preprint. Discussion started: 6 April 2020

Biogeosciences Discussions

Rainfall intensification increases the contribution of rewetting pulses to soil respiration

Stefano Manzoni[1,2], Arjun Chakrawal[1,2], Thomas Fischer[3], Joshua P. Schimel[4], Amilcare Porporato[5], Giulia Vico[6]

[1]Department of Physical Geography, Stockholm University, 10691 Stockholm, Sweden
[2]Bolin Centre for Climate Research, 10691 Stockholm, Sweden
[3]Central Analytical Laboratory, Brandenburg University of Technology, Cottbus, Germany
[4]Department of Ecology, Evolution, and Marine Biology, University of California, Santa Barbara, USA
[5]Department of Civil and environmental Engineering, Princeton University, Princeton, USA
[6]Department of Crop Production Ecology, Swedish University of Agricultural Sciences, Uppsala, Sweden

Correspondence to: Stefano Manzoni (stefano.manzoni@natgeo.su.se)

Abstract. Soil drying and wetting cycles promote carbon (C) release through large heterotrophic respiration pulses at rewetting, known as 'Birch' effect. Empirical evidence shows that drier conditions before rewetting and larger changes in soil moisture at rewetting cause larger respiration pulses. Because soil moisture varies in response to rainfall, also these respiration pulses depend on the random timing and intensity of precipitation. In addition to rewetting pulses, heterotrophic respiration continues during soil drying, eventually ceasing when soils are too dry to sustain microbial activity. The importance of respiration pulses in contributing to the overall soil respiration flux has been demonstrated empirically, but no theoretical investigation has so far evaluated how the relative contribution of these pulses may change along climatic gradients or as precipitation regimes shift in a given location. To fill this gap, we start by assuming that rewetting pulses and respiration rates during soil drying can be treated as random variables dependent on soil moisture fluctuations, and develop a stochastic model for soil heterotrophic respiration rates that analytically links the statistical properties of respiration to those of precipitation. Model results show that both the mean rewetting pulse respiration and the mean respiration during drying increase with increasing mean precipitation. However, the contribution of respiration pulses to the total heterotrophic respiration increases with decreasing precipitation frequency and to a lesser degree with decreasing precipitation depth, leading to an overall higher contribution of respiration pulses under future more intermittent and intense precipitation. Moreover, the variability of both components of soil respiration is also predicted to increase under these conditions. Therefore, our results suggest that with future more intermittent precipitation, respiration pulses and the associated nutrient release will intensify and become more variable, contributing more to soil biogeochemical cycling.

1. Introduction

Respiration pulses often occur after dry soils are wetted by rainfall or irrigation (Borken and Matzner, 2009; Daly et al., 2008; Jarvis et al., 2007; Kim et al., 2012). The respiration rates achieved at rewetting can be much higher than the rates maintained under permanently moist conditions, suggesting that the rewetting itself triggers a disproportionally high CO_2 production. Even if they are short-lived, these pulses can contribute a significant amount of the annual CO_2 release (Kim et al., 2012; Li et al., 2004; Yan et al., 2014). Their occurrence had been documented as long ago as Birch (1958)—for which the phenomenon has been named the 'Birch effect'—but they remain difficult to explain and predict.

Respiration pulses are larger when the change in soil moisture is larger and when the soil was drier before rewetting, as shown by observations under both laboratory (Birch, 1958; Fischer, 2009; Guo et al., 2014; Lado-Monserrat et al., 2014; Schaeffer et al., 2017; Williams and Xia, 2009) and field conditions (Cable et al., 2008; Carbone et al., 2011; Rubio and Detto, 2017; Unger et al., 2010; Yan et al., 2014). Several mechanisms have been postulated to explain these patterns (Kim et al., 2012; Schimel et al., 2007). It has been argued that cell lysis due to a rapid increase in water potential and subsequent consumption of the

https://doi.org/10.5194/bg-2020-95
Preprint. Discussion started: 6 April 2020

dead cells may cause the pulse (Bottner, 1985). Later measurements showed that little cell lysis occurs, but that intracellular materials (osmolytes) can be released at rewetting, contributing to the respiration pulse (Fierer and Schimel, 2003). However, in some soils microbial cells become dormant during drying rather than accumulating osmolytes (Boot et al., 2013). It is thus possible that respiration pulses are triggered by a physical process associated with the rewetting event—possibly re-establishment of hydrologic connectivity between substrates and microorganisms (Manzoni et al., 2016), or physical disruption of soil aggregates releasing old organic matter (Homyak et al., 2018). Indeed, there is a strong correlation between the CO_2 production after rewetting and the amount of dissolved organic carbon (DOC) consumed, suggesting that accumulated DOC could fuel the respiration pulse (Guo et al., 2014; Williams and Xia, 2009). It is likely that multiple mechanisms work in concert, shifting their relative importance under different conditions (Slessarev and Schimel, 2020).

The focus on the processes causing respiration pulses resulted in extensive work conducted under idealized laboratory conditions, in which soil moisture changes were controlled, typically following a regular pattern of drying and wetting (Fierer and Schimel, 2002; Miller et al., 2005; Shi and Marschner, 2014, 2015; Xiang et al., 2008). However, soil moisture varies randomly due to the stochastic nature of rainfall events (Katul et al., 2007; Rodriguez-Iturbe and Porporato, 2004). Two features of soil moisture dynamics are particularly important because they directly affect the intensity of a respiration pulse—the duration of dry periods and the soil moisture increment at rewetting. Therefore, experimental designs based on regular cycles of drying and wetting do not allow exploring how the stochastic nature of soil moisture fluctuations may affect respiration pulses.

To quantify how the long-term mean heterotrophic respiration varies as a function of rainfall statistical properties (duration of dry periods and intensity), we developed a stochastic soil moisture and respiration model, parameterized using available respiration data. Specifically, we ask—how does variability in rainfall translate in variability in respiration pulses? How does the long-term mean contribution of respiration pulses vary along climatic gradients? These questions are motivated by the hypothesis that respiration pulses contribute a larger proportion of soil respiration under climates with more intermittent and intense rainfall events, compared to climates in which soil moisture variations are mild. If that is the case, future climatic conditions characterized by longer droughts and more intense rainfall events are expected to increase the overall role of respiration pulses in ecosystem C budgets.

2. Methods

2.1. Theory

The theoretical framework is illustrated in Figure 1. We start from the premise that respiration follows changes in soil moisture during drying (R_d) and that respiration pulses occur immediately following rewetting. As such, respiration pulses depend on both the soil moisture at the end of the dry period and the soil moisture increase caused by rainfall (R_r). The stochasticity of rainfall timing and amount determines a range of possible durations of dry spells and soil moisture increments when rainfall occurs. As a result, respiration can be regarded as a stochastic process. To characterize statistically the two types of respiration, the statistical properties of both soil moisture and soil moisture changes at rewetting are needed. These statistical properties are included in the probability density function (PDF) of soil moisture, and the joint PDF of soil moisture and its increase at rewetting. Both distributions are derived in Section 2.1.1. The PDF of respiration rates during drying and respiration pulses at rewetting are derived in Sections 2.1.2 and 2.1.3, respectively. All symbols are defined in Table 1.

https://doi.org/10.5194/bg-2020-95
Preprint. Discussion started: 6 April 2020

2.1.1. Soil moisture dynamics

Soil moisture varies in response to rainfall events and the subsequent loss of soil water by deep infiltration below the rooting zone and evapotranspiration. The dynamics of soil moisture in the rooting zone (the most biogeochemically active) at the daily time scale can be described by the mass balance equation (Laio et al., 2001; Rodriguez-Iturbe and Porporato, 2004),

$$nZ_r \frac{ds}{dt} = P(t) - E(s(t)) - L(s(t), t), \quad (1)$$

where s is the saturation level (i.e., the relative volumetric soil moisture), n is the soil porosity, Z_r is the rooting depth, and P, E, and L represent precipitation inputs, evapotranspiration rate, and the combination of water losses due to deep percolation and surface runoff. Given our aim to describe the statistical properties of respiration rather than the details of soil moisture dynamics, we simplify the soil moisture mass balance equation to a form that is analytically tractable. Thus, we assume that evapotranspiration is the dominant water loss when soil moisture is lower than a threshold s_1 (equivalent to the soil field capacity), whereas runoff and deep percolation dominate above this threshold. Also, runoff and percolation are assumed to occur rapidly compared to the timescales of the soil dry-down (free drainage conditions), so that, after a precipitation event that brings soil moisture above the level s_1, soil moisture decreases instantaneously to s_1. For simplicity, evapotranspiration is modelled as a linear function of soil moisture (Porporato et al., 2004),

$$E = \frac{s - s_w}{s_1 - s_w} E_{max} = x E_{max}, \quad (2)$$

where E_{max} is the maximum rate of evapotranspiration, s_w is the plant wilting point (below which ET becomes negligible, and s_1 is the threshold above which runoff and percolation are dominant. In the second equality, a normalized soil moisture denoted by x is introduced to further simplify the notation. With these assumptions and definitions, s ranges between s_w and s_1, while the normalized soil moisture varies between 0 and 1.

Precipitation is treated as a marked Poisson process with mean frequency λ and rain-event depths exponentially distributed with mean α. At each rain event, soil moisture increases by an amount corresponding to the rain event depth (normalized by nZ_r), unless the depth exceeds the available soil storage capacity (i.e., $nZ_r(s_1 - s)$). Assuming that rainfall exceeding this capacity is routed to runoff, the PDF of soil moisture increments due to a rain event, y, for a given soil moisture at the end of the dry period, x_d, is given by (Laio et al., 2001)

$$p_y(y|x_d) = \theta[(1 - x_d) - y]\gamma e^{-\gamma y} + \delta[y - (1 - x_d)]e^{-\gamma(1 - x_d)}, \quad (3)$$

where $p_y(y|x_d)$ is the PDF of y *conditional* on soil moisture at the end of the dry period, x_d; $\theta[\cdot]$ is the Heaviside step function; $\delta[\cdot]$ is the Dirac delta function; and γ is a parameter group defined as $\gamma = \frac{nZ_r(s_1 - s_w)}{\alpha}$. The first term on the right-hand side of Eq. (3) represents the probability density of a soil moisture increase y equal to the rainfall depth ($\theta[\cdot]$ is equal to one for y<1-x_d; zero otherwise). The second term represents the probability of a soil moisture increase from the value x_d to the soil field capacity (x=1). This term is also referred to as an 'atom of probability' because $\delta[\cdot]$ is equal to zero for all soil moisture increments, except y=1-x_d, at which $\delta[\cdot] = \infty$.

With this stochastic description of precipitation events and further assuming stochastic steady state conditions, the PDF of the normalized soil moisture driven by the dynamics in Eq. (1) can be obtained analytically and reads (Porporato et al., 2004)

$$p_x(x) = C \frac{e^{-x\gamma} x^{-1+\frac{\lambda}{\eta}}}{\eta}, \quad (4)$$

where η is a parameter group defined as $\eta = \frac{E_{max}}{nZ_r(s_1 - s_w)}$. C is a normalization constant that guarantees that the area under $p_x(x)$ between x=0 and 1 is one,

$$C = \frac{\eta \gamma^{\frac{\lambda}{\eta}}}{\Gamma\left[\frac{\lambda}{\eta}\right] - \Gamma\left[\frac{\lambda}{\eta}, \gamma\right]}, \quad (5)$$

https://doi.org/10.5194/bg-2020-95
Preprint. Discussion started: 6 April 2020

where Γ[·] and Γ[·,·] are the complete and incomplete gamma functions (defined in Table 1). The PDF of soil moisture is the basis to obtain the PDF of respiration during soil drying (Section 2.1.2).

The last distribution needed to calculate the statistical properties of soil respiration pulses (Section 2.1.3) is the joint PDF of soil moisture at the end of a dry period and soil moisture increase due to precipitation events, denoted by $p_{y,x_d}(y,x_d)$ (note that both y and x_d are stochastic variables in this joint PDF). Thanks to the properties of the Poisson process, the PDF of soil moisture at the end of the dry period is equal to the PDF of soil moisture at a generic time (Cox and Miller, 2001); i.e., $p_{x_d}(x_d) = p_x(x)$. Because precipitation does not depend on antecedent soil moisture conditions in this model, the PDF of soil moisture at the end of a dry period is independent of the PDF of the subsequent precipitation event and soil moisture increase. Thus, the joint PDF of x_d and y is given by the product of the PDFs of x_d (Eq. (4)) and of y (Eq. (3)),

$$p_{y,x_d}(y,x_d) = p_x(x_d)p_y(y|x_d). \quad (6)$$

2.1.2. Respiration during soil drying

During a dry period, the heterotrophic respiration rate decreases in response to the gradual decrease in soil moisture, following a concave-downward trend (Manzoni et al., 2012; Moyano et al., 2012). Consistent with the hydrologic model setup, we assume that the soil drains rapidly and hence does not remain under saturated conditions long enough to develop anoxic conditions. It is thus reasonable to assume that respiration declines between the soil field capacity (equivalent to s_1 in this model) and a lower soil moisture threshold for microbial activity. This lower threshold corresponds to water potential levels around -15 MPa in sieved soil samples (Manzoni and Katul, 2014), but here we assume that respiration becomes much smaller than rates under well-watered conditions already at the plant wilting point s_w; i.e., at a water potential of -1.5 MPa. This assumption is motivated by the observation that in intact soil cores and under field conditions respiration stops in wetter conditions than at -15 MPa (e.g., -2.7 MPa (Carbone et al., 2011)). Moreover, this allows keeping the parameter number to a minimum, consistent with the minimal soil moisture balance model of Eq. (1) and (2) and the overall idealized representation of soil heterotrophic respiration. The respiration decline with a lower threshold s_w (corresponding to x=0) can be captured by a parabolic relation,

$$R_d = R_{d,max}(2x - x^2), \quad (7)$$

where R_d and $R_{d,max}$ respectively denote the respiration rate during drying and the maximum respiration rate in the absence of rapid rewetting (i.e., R_d at x=1 or s=s_1). Using other monotonic and concave-downward relations between respiration and soil moisture would not qualitatively alter the results.

In Eq. (1), soil moisture is a random variable, whose PDF follows Eq. (4). Therefore, R_d from Eq. (7) is also a random variable, which can be obtained from the PDF of soil moisture using the derived distribution approach (Kottegoda and Rosso, 1998),

$$p_{R_d}(R_d) = p_x\big(x(R_d)\big)\left|\frac{dx}{dR_d}\right|, \quad (8)$$

where on the right-hand side soil moisture is expressed as a function of R_d by inverting Eq. (7),

$$x(R_d) = 1 - \sqrt{1 - \frac{R_d}{R_{d,max}}}. \quad (9)$$

In turn, Eq. (9) allows calculating the slope of the $x(R_d)$ relation, which is also needed in Eq. (8),

$$\frac{dx}{dR_d} = \left(2R_{d,max}\sqrt{1 - \frac{R_d}{R_{d,max}}}\right)^{-1}. \quad (10)$$

The PDF of R_d is thus obtained from Eq. (8)-(10) as

$$p_{R_d}(R_d) = C\frac{e^{-\gamma\left(1-\sqrt{1-r_d}\right)}\left(1-\sqrt{1-r_d}\right)^{-1+\frac{\lambda}{\eta}}}{\eta 2R_{d,max}\sqrt{1-r_d}}, \quad (11)$$

https://doi.org/10.5194/bg-2020-95
Preprint. Discussion started: 6 April 2020

where the normalized respiration $r_d = \frac{R_d}{R_{d,max}}$ is introduced to simplify the notation. This PDF can now be used to calculate analytically the long-term mean of R_d, denoted by $\langle R_d \rangle$,

$$\langle R_d \rangle = \frac{R_{d,max} C'}{\gamma^2} \left\{ \Gamma\left[2 + \frac{\lambda}{\eta}, \gamma\right] - 2\gamma\Gamma\left[1 + \frac{\lambda}{\eta}, \gamma\right] - \frac{\lambda(\eta - 2\gamma\eta + \lambda)}{\eta^2} \Gamma\left[\frac{\lambda}{\eta}\right] \right\}, \quad (12)$$

where for convenience the parameter group $C' = \left(\Gamma\left[\frac{\lambda}{\eta}\right] - \Gamma\left[\frac{\lambda}{\eta}, \gamma\right]\right)^{-1}$ is defined. The standard deviation of R_d, denoted by σ_{R_d}, can not be obtained analytically, but it can be calculated through numerical integration of Eq. (11).

2.1.3. Respiration pulses at rewetting

Respiration pulses at rewetting are caused by mineralization of available C and microbial products at the end of the dry period, which in turn depend on how intense the rewetting event was. As a result of these processes, in a given soil, rewetting events depend on both soil moisture before the rewetting x_d, and the change in soil moisture y (Birch, 1958; Lado-Monserrat et al., 2014). This relation can be captured by the empirical function (justified and parameterized in Section 2.2.1),

$$R_r = R_{r,max} \frac{y}{1 + \frac{x_d}{b}} \theta[(1 - x_d) - y], \quad (13)$$

where $R_{r,max}$ is the largest respiration pulse possible (achieved when y=1 and x_d=0), and b is a parameter weighing the effect of antecedent soil moisture conditions. The last term in Eq. (13) is a Heaviside function limiting the relation between R_r and y to conditions in which soil moisture at most fills the available pore space (as in Eq. (3), $\theta[\cdot]$ is equal to one only when $y < 1 - x_d$). If before the rain event soil moisture is at the plant wilting point (x_d=0) and the precipitation event is sufficient to reach s_1 (i.e., $y = x - x_d = 1$), the maximum respiration pulse is attained and R_r=$R_{r,max}$. Here, R_r represents an amount of C respired when the rewetting event occurs, so its dimensions differ from those of the respiration rate during drying, R_d; these two quantities are combined in the total respiration rate in Section 2.1.5.

Because both y and x_d are random variables that follow the PDF of Eq. (6), also R_r should be regarded as a random variable following its own PDF. Different from the PDF of R_d, which was obtained from the univariate PDF of soil moisture, the PDF of R_r has to be derived from the joint PDF of y and x_d. The derived distribution approach can still be used, but it requires the determinant of the Jacobian matrix of the transformation from y and x_d to R_r (Kottegoda and Rosso, 1998). To proceed, it is first convenient to introduce an auxiliary variable X=x_d, which is used together with Eq. (13) to find the transformation from the original variables y and x_d to R_r and X,

$$\begin{cases} X = x_d \\ R_r = R_{r,max} \frac{y}{1 + \frac{x_d}{b}} \end{cases} \Rightarrow \begin{cases} x_d = X \\ y = \frac{R_r}{R_{r,max}} \left(1 + \frac{X}{b}\right) \end{cases} \quad \text{for} \quad y < 1 - x_d, \quad (14)$$

where the inequality limits the soil-moisture increments as the Heaviside function in Eq. (13). Second, the system on the left of Eq. (14) is inverted to express the original variables as a function of the transformed variables (reported on the right of Eq. (14)), similar to the inversion done in Eq. (9). Third, we calculate the Jacobian matrix,

$$J = \begin{bmatrix} \frac{\partial x_d}{\partial X} & \frac{\partial x_d}{\partial R_r} \\ \frac{\partial y}{\partial X} & \frac{\partial y}{\partial R_r} \end{bmatrix} = \begin{bmatrix} 1 & 0 \\ \frac{R_r}{R_{r,max}} \frac{1}{b} & \frac{1}{R_{r,max}} \left(1 + \frac{X}{b}\right) \end{bmatrix}, \quad (15)$$

and the determinant of the Jacobian,

$$|J| = \frac{1}{R_{r,max}} \left(1 + \frac{X}{b}\right). \quad (16)$$

Fourth, the joint PDF of the variables X and R_r is obtained using the derived distribution approach,

$$p_{X,R_r}(X, R_r) = p_{y,x_d}\left(y(X, R_r), x_d(X, R_r)\right)|J|, \quad (17)$$

https://doi.org/10.5194/bg-2020-95
Preprint. Discussion started: 6 April 2020

where as in Section 2.1.2 all the terms on the right-hand side only depend on X and R_r, and p_{y,x_d} is given by Eq. (6). Finally, to obtain the (marginal) PDF of R_r, the joint PDF in Eq. (17) is integrated over all possible values of X,

$$p_{R_r}(R_r) = \int_0^1 p_{X,R_r}(X, R_r)\, dX = \\ = \frac{C'}{(b+r_r)R_{r,max}}\left\{e^{-\gamma}\left[\frac{\gamma(1-r_r)}{1+\frac{r_r}{b}}\right]^{\frac{\lambda}{\eta}}\frac{1+b}{1-r_r} + \right. \\ \left. e^{-\gamma r_r}\left(\frac{1}{1+\frac{r_r}{b}}\right)^{\frac{\lambda}{\eta}}\left[\gamma(b+r_r)\left(\Gamma\left[\frac{\lambda}{\eta}\right] - \Gamma\left[\frac{\lambda}{\eta}, \gamma(1-r_r)\right]\right) + \Gamma\left[1+\frac{\lambda}{\eta}\right] - \Gamma\left[1+\frac{\lambda}{\eta}, \gamma(1-r_r)\right]\right]\right\}, \quad (18)$$

where on the right hand side the normalized respiration pulse $r_r = \frac{R_r}{R_{r,max}}$ is introduced to simplify the notation, and as before $C' = \left(\Gamma\left[\frac{\lambda}{\eta}\right] - \Gamma\left[\frac{\lambda}{\eta}, \gamma\right]\right)^{-1}$. Due to the complexity of Eq. (18), the long-term mean and standard deviation of R_r, respectively denoted by $\langle R_r \rangle$ and σ_{R_r}, need to be obtained via numerical integration of the PDF of R_r.

2.1.4. Rewetting pulses only dependent on soil moisture change

It is useful to consider respiration pulses that only depend on the soil moisture increments; i.e., $b \gg x_d$. In this case, Eq. (13) reduces to $R_r = yR_{r,max}$ (i.e., $y = R_r/R_{r,max}$)—equivalent to having always a completely dry soil before rewetting. Thanks to the simplicity of the respiration pulse equation, $p_{R_r}(R_r)$ can be obtained as a derived distribution from the marginal PDF of the soil moisture changes y,

$$p_y(y) = \int_0^1 p_y(y|x_d)dx_d = [1 + \gamma(1-y)]e^{-y\gamma}, \quad (19)$$

where $p_y(y|x_d)$ is from Eq. (3). The $p_{R_r}(R_r)$ is then obtained as,

$$p_{R_r}(R_r) = p_y\big(y(R_r)\big)\left|\frac{dy}{dR_r}\right| = \frac{1+\gamma\left(1-\frac{R_r}{R_{r,max}}\right)}{R_{r,max}}e^{-\frac{\gamma R_r}{R_{r,max}}}. \quad (20)$$

Thanks to the simplicity of Eq. (20), in this particular case the long-term mean and standard deviation of the respiration pulses are found analytically,

$$\langle R_r \rangle = \frac{R_{r,max}}{\gamma^2}(e^{-\gamma} + \gamma - 1), \quad (21)$$

$$\sigma_{R_r} = \frac{R_{r,max}}{\gamma^2}\sqrt{(\gamma-2)\gamma - 1 + 2e^{-\gamma}(1+\gamma+\gamma^2) - e^{-2\gamma}}. \quad (22)$$

Thus, when respiration pulses are simply proportional to the soil moisture change at rewetting, their mean only depends on the maximum pulse size $R_{r,max}$ and the ratio of soil water storage capacity and mean precipitation depth (i.e., the parameter group $\gamma = \frac{nZ_r(s_1 - s_w)}{\alpha}$).

2.1.5. Combining respiration during soil drying and at rewetting

The total mean heterotrophic respiration rate is given by the sum of the mean respiration rate during soil drying $\langle R_d \rangle$ (Eq. (12); expressed in gC m^{-2} d^{-1}) and the mean rate of respiration resulting from the sequence of rewetting pulses over the study period (denoted by $\langle R_r^* \rangle$ and also expressed in gC m^{-2} d^{-1}). The $\langle R_r^* \rangle$ is calculated as the mean amount of respired carbon ($\langle R_r \rangle$ from Eq. (18), expressed in gC m^{-2}) divided by the mean rainfall inter-arrival time, $1/\lambda$,

$$\langle R_r^* \rangle = \lambda \langle R_r \rangle. \quad (23)$$

The mean total heterotrophic respiration rate is then obtained as,

$$\langle R_t \rangle = \langle R_d \rangle + \langle R_r^* \rangle. \quad (24)$$

https://doi.org/10.5194/bg-2020-95
Preprint. Discussion started: 6 April 2020

In what follows, the ratio of respiration pulse to total respiration (i.e., $\langle R_r^* \rangle / \langle R_t \rangle$) will also be considered, to evaluate the overall contribution of respiration pulses.

2.2. Data analysis

2.2.1. Laboratory incubation data for model calibration

The phenomenological respiration models in Eq. (7) and (13) require knowledge of three parameters: the respiration rate at the soil field capacity ($R_{d,max}$), the maximum respiration pulse size ($R_{r,max}$), and the sensitivity of the respiration pulse to the initial soil moisture (b). To estimate these three parameters, we selected datasets where both the soil moisture before rewetting and the soil moisture increments were manipulated (Fischer, 2009; Guo et al., 2014; Lado-Monserrat et al., 2014). All data reported in these three publications were used, except data from the litter-amended soils in Lado-Monserrat et al. (2014) (we chose to focus on 'natural' conditions) and data from small (y<0.3) rewetting events in Fischer (2009) (they exhibited small respiration peaks despite nearly stable soil moisture). The reported respiration amounts at rewetting were corrected to isolate the pulse size (R_r) from the respiration that would have occurred at constant soil moisture (R_d). This was done by calculating $R_{d,max}$ from control soil samples kept constantly wet (Guo et al., 2014) or from the post-pulse respiration rate before soil moisture started to decline in experiments where drying was allowed in all samples (Lado-Monserrat et al., 2014). In contrast, respiration pulses had already been isolated by Fischer (2009). The last step of the parameter estimation involved fitting Eq. (13) to the data using a nonlinear least square algorithm (*fminunc* function in Matlab).

Because respiration amounts and rates in these laboratory incubations were expressed respectively in μg g^{-1} and μg g^{-1} d^{-1} (or on a per unit soil organic C basis), units were converted to g m^{-2} and g m^{-2} d^{-1} using bulk densities and sampling depths reported in the original publications (results are shown in Table 2).

2.2.2. Field data for model validation

In addition to estimating the values of the three parameters in Eq. (7) and (13), we validated the results from the whole stochastic model by comparting the predicted long-term mean heterotrophic respiration rates to observations along a rainfall manipulation gradient in a semi-arid steppe (Zhang et al., 2017b, 2019). Briefly, the precipitation gradient was established by excluding 30% and 60% of precipitation with rain shelters, and by increasing precipitation by 30% and 60% through irrigation. By design, only precipitation amounts (not timing) were altered, resulting in five mean rainfall depths α =2.6, 3.9, 5.1, 6.4, and 7.6 mm. Mean evapotranspiration rates, soil moisture, and heterotrophic respiration rates along the rainfall gradient were obtained from the published supplementary materials in Zhang et al. (2019) or from the Dryad dataset by Zhang et al. (2017a). Hydrologic parameters that were not provided were estimated as follows. The maximum evapotranspiration rate (assumed equal the potential evapotranspiration) and the mean rainfall frequency were estimated from May-August CRU data at the rainfall manipulation site (E_{max}=4.3 mm d^{-1} and λ=0.41 d^{-1}). The soil at the site has sandy loam texture (Bingwei Zhang, personal communication) and soil properties were obtained accordingly: n=0.42, s_w=0.11, s_1=0.52 (Table 2.1 in Rodriguez-Iturbe and Porporato, 2004). Finally, the rooting depth Z_r=0.2 m was estimated as the soil depth above which approximately 70% of belowground productivity occurs, based on data from Zhang et al. (2020).

Regarding the parameters of the rewetting respiration function (Eq. (13)), we assumed $R_{d,max}$=2 gC m^{-2} d^{-1} and b=0.1. These values are deemed reasonable for mineral soils based on Table 2, and accounting for a rooting depth about double the sampling depth of the incubation experiments (which doubles the $R_{d,max}$ values in Table 2). Without specific information on respiration pulse sizes, we let $R_{r,max}$ vary over a wide range. Additionally, we tested the simplified respiration model (Section 2.1.4), which does not require any assumption on b, against the same total heterotrophic respiration dataset.

https://doi.org/10.5194/bg-2020-95
Preprint. Discussion started: 6 April 2020

3. Results

3.1. Dependence of rewetting respiration on soil moisture

Laboratory incubation data were used to parameterize the functions linking respiration to soil moisture. As expected, the respiration pulses at rewetting depend on both rewetting intensity (y) and pre-wetting soil moisture (x_d), and this relation is well-characterized by Eq. (13) (Figure 2; Table 2). In general, mineral soils exhibit much lower respiration pulses than do organic soils, though values are more comparable if respiration is normalized by soil organic C, rather than soil dry weight. Consistent with this trend, both $R_{r,max}$ and $R_{d,max}$ are higher in the organic soils, and so is the ratio between $R_{r,max}$ and $R_{d,max}$. The sensitivity parameter b shows milder variation across soils than the other parameters, with an average value $b \approx 0.1$. Based on this data analysis, in the following theoretical exploration we set parameter values intermediate between the extremes reported in Table 2 to ensure reasonable results (i.e., $R_{r,max}$=5 gC m^{-2}, $R_{d,max}$=1 gC m^{-2} d^{-1}, and b=0.1).

3.2. General model behaviour

Figure 3 shows two examples of the simulated trajectories of soil moisture and respiration, for contrasting climatic conditions (more frequent precipitation in the left panels than in the right panels). It is important to note that in this comparison across climatic conditions (and in the comparisons that follow), the maximum respiration $R_{r,max}$ and $R_{d,max}$ are fixed, while in reality they are likely proportional to soil organic C availability, which in turn is the result of a long-term and soil moisture-dependent balance between C inputs from vegetation and respiration (this limitation is discussed in Section 4.2). Respiration rates during dry periods follow soil moisture changes, declining as soil dries and returning to higher levels at rewetting (Figure 3b, f). In addition to this rewetting-induced restoration of high respiration rates, rewetting causes CO_2 emission pulses, represented by vertical bars. Under the wetter climate (Figure 3b), respiration pulses are more frequent than under the dry climate (Figure 3f) because of the higher precipitation frequency. However, most of the respiration pulses are small because soil moisture increments at rewetting are often limited by the available soil pore space and a relatively large fraction of precipitation is lost to runoff and deep percolation. In contrast, under dryer conditions, changes in soil moisture are large because on average soil moisture is low and the pore space is rarely filled up completely. As a result, the fewer respiration pulses are larger under dry than under wet conditions.

The bottom panels in Figure 3 show the PDF of respiration for the same two climatic conditions analysed in the upper panels. While the PDF of R_r is positively skewed regardless of climate (but with heavier tails under dry conditions, Figure 3c, g), the PDF of R_d is strongly affected by climatic conditions—the probability of high values for R_d is higher under wet conditions (negatively skewed PDF) and lower under dry conditions (positively skewed PDF, Figure 3d, h). This pattern is caused by the prevalence of high soil moisture values in the wet climate scenario, which maintain relatively high R_d. Figure 3c, d, g, h also show that the theoretical PDF (Eq. (11) and (18)) match perfectly the distribution of the numerically simulated data. The shape of the theoretical PDF of R_d in Figure 3h might seem incorrect, as it increases sharply at high respiration values. This increase is due to the flat derivative of the R_d-soil moisture relation (Eq. (7)), which causes an asymptote in the PDF at R_d=$R_{d,max}$ (Eq. (11)). However, the area under this spike is vanishingly small when climatic conditions are dry as in the example of Figure 3e-h, so that it is highly unlikely to have any respiration value around $R_{d,max}$.

3.3. Model test under field conditions

Field data were used to test if the hydrologic and soil respiration models could capture trends in the mean evapotranspiration and heterotrophic respiration along a precipitation gradient (Figure 4). The trend of the mean evapotranspiration rate with increasing mean rainfall depth was captured reasonably well (Figure 4a), considering that no formal calibration was conducted, and all parameters were estimated based on independent information. Similarly, the model correctly predicts the trend in soil

https://doi.org/10.5194/bg-2020-95
Preprint. Discussion started: 6 April 2020

moisture (not shown), but with an overestimation bias around 0.05-0.1 (in terms of normalized soil moisture x). This overestimation is expected, because soil moisture had been measured in the drier top 0.1 m of soil, while the model considers average soil moisture over a 0.2 m depth. Also the trend in total heterotrophic respiration is predicted correctly by the full model, which explains 77% of the variance in the respiration data (black curve in Figure 4b). Calibrating the two parameters of Eq. (13) and $R_{d,max}$ would allow a better fit, but since the goal here is to provide a qualitative model validation and not a quantitative performance assessment, we deem the model suitable for the following theoretical analyses.

We also tested the simpler version of the model, in which respiration pulses only depend on the soil moisture increment. Without the effect of pre-wetting soil moisture, this version predicts higher mean respiration than the full model (red lines in Figure 4b), and higher contribution of rewetting respiration to the total heterotrophic respiration (red lines in Figure 4c).

3.4. Dependence of respiration on rainfall statistical properties

Figure 5 shows the predicted effect of precipitation regimes on heterotrophic respiration during drying and at rewetting (Figure 5a, b), on the total respiration rate (Figure 5c), and on the fraction of total heterotrophic respiration contributed by rewetting pulses (Figure 5d). As in Figure 3, $R_{r,max}$ and $R_{d,max}$ are fixed to focus on the role of climatic conditions, so the patterns shown in Figure 5a-c should be interpreted as changes of mean respiration rates along gradients of precipitation frequency (λ) and mean depth (α) for given soil organic C stocks. In contrast, results in Figure 5d can be generalized to soils with contrasting C stocks, because the relative contribution of respiration pulses to the total respiration is less dependent on the organic C availability than the mean respiration rates.

Because in this minimal model the mean precipitation rate is given by $\langle P \rangle = \alpha\lambda$, precipitation can be increased by assuming more frequent rain events (i.e., increasing λ), deeper events (i.e., increasing α), or both. Any of these changes increase mean respiration during drying and at rewetting (Figure 5a, b). As $\langle R_d \rangle$ and $\langle R_r^* \rangle$ increase with precipitation, the relative contribution of respiration pulses to the total respiration rate, $\langle R_r^* \rangle / \langle R_t \rangle$, tends to decrease from drier to wetter conditions, especially when rain events become more frequent (as opposed to more intense) (Figure 5d). This pattern is caused by the relatively larger respiration pulses occurring when soils are dry and rewetting causes large soil moisture increments (compare examples in Figure 3b and 3f). Moreover, the relative change of $\langle R_r^* \rangle / \langle R_t \rangle$ is smaller than the change in $\langle R_d \rangle$ or $\langle R_r^* \rangle$ as precipitation regimes are varied.

Not only the mean respiration rates vary with hydro-climatic conditions, but also the variability of both respiration rates during drying and respiration pulses at rewetting (Figure 6). The standard deviation of R_d exhibits maxima at intermediate α when λ is fixed, and at intermediate λ when α is fixed (Figure 6a). This pattern is due to a shift in the shape of the PDF of R_d when moving from dry to wet conditions. Under dry conditions, the PDF of R_d has relatively low variance and is negatively skewed (Figure 3d); as conditions become wetter the PDF flattens and the variance increases, and finally under wet conditions the PDF transitions again to a low-variance, but positively skewed PDF (Figure 3h). In contrast, the PDF of R_r is always positively skewed with variance decreasing with increasing wetness (Figure 6b; compare examples in Figure 3c and g). The decrease in variance occurs both when increasing α and when increasing λ.

The coefficients of variation (CV) of R_d and R_r—which are expected to be less affected by variations in organic C availability along climatic gradients—vary less than the corresponding standard deviations and tend to decrease as conditions move from dry to wet (Figure 6c, d). Specifically, the CV of R_d decreases with both increasing λ and increasing α. In contrast, the CV of R_r is nearly independent of α, but decreases with increasing λ.

https://doi.org/10.5194/bg-2020-95
Preprint. Discussion started: 6 April 2020


Biogeosciences Discussions Open Access EGU

4. Discussion

Heterotrophic respiration fluctuates at multiple temporal scales in response to hydro-climatic variability (Messori et al., 2019; Rubio and Detto, 2017)—from inter-annual variations due to climatic anomalies and extreme events (Reichstein et al., 2013), to seasonal variations partly linked to plant activity (Zhang et al., 2018), to short-term fluctuations induced by soil drying and rewetting (Daly et al., 2009). Here we focus on respiration fluctuations during drying-wetting cycles, and how they are affected by precipitation regimes. Differently from most other modelling approaches to describe these dynamics, we develop a probabilistic model with analytical solutions for the probability density function of respiration rate (discussed in Section 4.1). For the sake of analytical tractability, this model rests on important assumptions (Section 4.2), but despite its simplicity has the potential to assess the effect of precipitation variability (and its expected changes) on heterotrophic respiration (Section 4.3).

4.1. Comparison with previous stochastic approaches

Most biogeochemical models assume that respiration (and other processes) depend on a generic soil property φ following an empirical function $f(\varphi)$ (Bauer et al., 2008; Moyano et al., 2013). As φ changes through time (e.g., soil moisture and temperature), also the biogeochemical rate associated with φ varies. Thus, the biogeochemical models use the function $f(\varphi)$ to convert measured time series of soil moisture and other environmental variables into biogeochemical rates. The different approach we follow here consists in linking a known probability density of φ, to the probability density of the function $f(\varphi)$ to capture the propagation of the statistical properties of φ to $f(\varphi)$. This can be done by the derived distribution approach, as in Eq. (8). This approach has been used to investigate gaseous nitrogen emissions in response to soil moisture fluctuations (Ridolfi et al., 2003), but the only example studying soil respiration rate we are aware of focused on respiration responses to temperature fluctuations (Sierra et al., 2011). These approaches provide simple and mathematically elegant solutions, but have so far been limited to the effect of a single driver of the biogeochemical flux of interest. Respiration responses to soil moisture are more complex because rewetting pulses depend on both soil moisture increment and pre-wetting soil moisture (Figure 2), requiring the solution of a bivariate stochastic process. Thus, our approach—by accounting for both these effects—is more general and applicable along gradients where the statistical properties describing the precipitation regime vary significantly (Figure 4).

A previous stochastic approach focused on the CO_2 concentration in the pore space instead of respiration rates (Daly et al., 2008). Observations suggest that CO_2 concentration responds to a rainfall event with a sudden increase at rewetting, followed by a decrease approximated by a negative exponential function. This dynamic can be described as a stochastic process where CO_2 concentration is the random variable and precipitation represents the stochastic forcing (Daly et al., 2008). With this approach, the long-term mean CO_2 concentration was found to depend on the average rainfall rate ($\lambda\alpha$), while the standard deviation of CO_2 concentration depends on $\lambda\alpha^2$. This indicates that rainfall intensity (in terms of mean event depth α) plays a more important role than rainfall frequency in driving the variability of soil CO_2 concentration. Soil respiration was shown to be approximately proportional to CO_2 concentration in the pore space over a broad range of concentrations (Daly et al., 2008), so that respiration statistics are also expected to scale with rainfall statistics in the same way as soil CO_2 concentrations. This result is consistent with our finding that all components of heterotrophic respiration increase with both λ and α (Figure 5).

4.2. Methodological limitations

Two model assumptions can alter the interpretation of our results: first, that respiration pulses can be regarded as instantaneous, and second, that the two parameters $R_{d,max}$ and $R_{r,max}$ are independent of climatic conditions.

https://doi.org/10.5194/bg-2020-95
Preprint. Discussion started: 6 April 2020

Respiration pulses are modelled as instantaneous events of CO_2 emission with a given size (Section 2.1.3). While mathematically convenient, rewetting respiration pulses are known to last for a few days after the rewetting has ended. Indeed, when analysing laboratory incubation data, the pulse size is generally calculated by integrating through time the respiration rates above the rate occurring at stable soil moisture. The integration window ranges between two and three days (e.g., Fischer, 2009). This simplified approach to separate the actual rewetting pulse from the respiration rate at stable soil moisture requires some caution when rainfall events are frequent. In that case, pulses would overlap rather than being distinct. Moreover, with frequent rainfall, respiration could be inhibited due to water logging (Moyano et al., 2013; Rubio and Detto, 2017), and no respiration pulse might occur. Thus, to avoid these issues, our equations should not be used in wet environments with $\lambda > 0.3$ d^{-1}.

We calculated the statistical properties of the respiration rate, but did not consider the dynamics of the soil organic matter and plants that supply resources for microbial growth and respiration. Widely different precipitation amounts and distributions such as those depicted in Figures 5 and 6 are associated with different plant communities, whose productivity increases along gradients of precipitation (Huxman et al., 2004; Luyssaert et al., 2007), providing litter and root exudates whose C is eventually stabilized into soil organic matter. Indeed soil organic carbon stocks increase with increasing mean annual precipitation (Guo et al., 2006). Hence, soil organic matter probably varies along the axes of Figures 5 and 6, which are instead interpreted here as purely climatic gradients. Such variations in organic matter content would affect the maximum respiration rates and pulse size, $R_{d,max}$ and $R_{r,max}$ (e.g., compare mineral and organic soils in Table 2). Because the mean respiration rates scale with the maximum rates (as apparent analytically from Eq. (21)), it is reasonable to expect that higher organic matter content along precipitation gradients increases the sensitivity of respiration to changes in precipitation compared to predictions in Figure 5. Moreover, soil C substrates might be depleted through multiple drying and rewetting events—a behaviour we do not consider in the proposed statistically stationary model. While some experiments show sustained rewetting pulses (Miller et al., 2005; Xiang et al., 2008), others show reduced total respiration with increasing frequency of drying and rewetting, possibly due to substrate depletion (Shi and Marschner, 2014). To capture these dynamics, a more complex model describing the changes in substrate and microbial compartments would be needed (e.g., Brangarí et al., 2018; Lawrence et al., 2009) at the cost of losing the analytical tractability.

4.3. How are the statistical properties of heterotrophic respiration varying with changing precipitation regimes?

The axes of Figures 5 and 6 can be interpreted in terms of changes in precipitation patterns caused by ongoing climatic changes. If rainfall in a semi-arid or mesic environment increases (due to either more frequent or larger events), heterotrophic respiration also increases (Yan et al., 2014; Zhang et al., 2019)—this is not surprising as soils become on average wetter, removing water limitation and promoting microbial activity. However, the variability in respiration does not always change monotonically with increasing rainfall. Figure 6b shows that the standard deviation of the respiration pulses increases with more intense (higher α) and less frequent (lower λ) rainfall. In contrast, the standard deviation of the respiration rate during drying, R_d, peaks at intermediate α and λ, and declines thereafter because the respiration response is flat and thus have higher variance at intermediate wetness (Eq. (7); Figure 6a). Nevertheless, when α and λ are changed simultaneously (moving along the white curves in Figures 5-6), the mean and standard deviation of both respiration components increase with more intermittent and intense rainfall events. Therefore, higher precipitation as driven by increasing α or λ is expected to increase the respiration pulses (Figures 5b), while decreasing their contribution to the total heterotrophic respiration (Figure 5d).

It is perhaps more interesting to understand respiration responses to changes in rainfall patterns for given total rainfall amounts. In experimental rainfall manipulations that mimic the predicted climatic changes, increased variability in soil moisture associated with more intense but less frequent precipitation events decreases total soil respiration (Harper et al., 2005). This observation appears to be at odds with our result that the mean total respiration slightly increases when precipitation becomes more intermittent while maintaining a given mean precipitation rate (i.e., moving right to left along one of the white curves in

https://doi.org/10.5194/bg-2020-95
Preprint. Discussion started: 6 April 2020

Figure 5). Our result is explained by the concavity of the relation between respiration and soil moisture during drying (Figure 1), which causes the early phase of soil drying after a large precipitation event to have a large effect on the mean respiration. In other words, few large rainfall events that saturate the soil play a more important role than many small events. Moving left along the white curves of Figure 5, precipitation becomes less frequent, but the average precipitation depth increases, which amplifies this effect causing $\langle R_d \rangle$ (Figure 5b), and also $\langle R_t \rangle$ (Figure 5c), to increase. However, our approach neglects the lower plant C inputs and contributions to total soil respiration under this more challenging precipitation regime (Harper et al., 2005), which likely explains the observed reduction in total (combined autotrophic and heterotrophic) respiration rate.

We also found that the contribution of rewetting pulses to the total heterotrophic respiration increases when rainfall becomes more intermittent and rainfall events larger (again moving left along the white curves in Figures 5-6). This result is consistent with observations in a temperate steppe (Yan et al., 2014). We can thus surmise that climatic changes causing longer dry period and more intense rainfall events (IPCC, 2012) will increase the role of pulse responses, including not only respiration, but also nitrogen mineralization pulses that could release nitrogen at a time when plant uptake is low. In turn, this can cause a de-coupling of nitrogen supply and demand, with possible negative consequences for ecosystem productivity (Augustine and McNaughton, 2004; Dijkstra et al., 2012).

5. Conclusions

Heterotrophic respiration depends nonlinearly on soil moisture—not only does it follow soil moisture during a dry period, but it also responds rapidly to rewetting. These rewetting responses occur in the form of pulses of CO_2 whose size increases with increasing soil moisture increment and decreasing pre-wetting soil moisture. We used this relation between respiration pulses and soil moisture to characterize analytically the statistical properties of respiration rates as a function of the statistical properties of the rainfall events that drive the soil moisture changes. Consistent with empirical evidence, our model predicts that dryer climatic conditions (either lower rainfall depths or longer dry periods between two rain events) lower total heterotrophic respiration. More interestingly, we showed that the contribution of rewetting pulses to the total heterotrophic respiration increases in dryer climates, but also when the precipitation regimes shift towards more intermittent and intense events (even at constant total average rainfall). Therefore, our results suggest that the expected intensification of precipitation will increase the role of rewetting respiration pulses in the ecosystem C budgets.

Data availability

All data used in this study are published and available in the original publications and linked supplementary materials (see Table 2 for references on the laboratory data and Section 2.2.2 for references on the field data).

Author contributions

SM and GV conceptualized the study; SM, GV, and AP developed the theory; TF provided and discussed data; AC analysed data and prepared Fig. 2; SM prepared the other figures and drafted the manuscript; all authors discussed the study ideas, and read and commented the manuscript.

Competing interests

The authors declare that they have no conflict of interest.

https://doi.org/10.5194/bg-2020-95
Preprint. Discussion started: 6 April 2020

Acknowledgements

This work was supported by the Swedish Research Council Vetenskapsrådet (grant 2016-04146) and Formas (grants 2018-00968 and 2018-00425). GV was partially supported by the Swedish Research Council Vetenskapsrådet (grant 2016-04910). We thank Antonio L. Lidón and Bingwei Zhang for sharing data and assisting in their interpretation.

References

Augustine, D. J. and McNaughton, S. J.: Temporal asynchrony in soil nutrient dynamics and plant production in a semiarid ecosystem, Ecosystems, 7(8), 829–840, 2004.

Bauer, J., Herbst, M., Huisman, J. A., Weihermuller, L. and Vereecken, H.: Sensitivity of simulated soil heterotrophic respiration to temperature and moisture reduction functions, Geoderma, 145(1–2), 17–27, 2008.

Birch, H. F.: The effect of soil drying on humus decomposition and nitrogen availability, Plant Soil, 10(1), 9–31, 1958.

Boot, C. M., Schaeffer, S. M. and Schimel, J. P.: Static osmolyte concentrations in microbial biomass during seasonal drought in a California grassland, Soil Biol. Biochem., 57(0), 356–361, doi:10.1016/j.soilbio.2012.09.005, 2013.

Borken, W. and Matzner, E.: Reappraisal of drying and wetting effects on C and N mineralization and fluxes in soils, Glob. Change Biol., 15(4), 808–824, 2009.

Bottner, P.: Response of Microbial Biomass to Alternate Moist and Dry Conditions in a Soil Incubated with C-14-Labeled and N-15-Labelled Plant-Material, Soil Biol. Biochem., 17(3), 329–337, 1985.

Brangarí, A. C., Fernàndez-Garcia, D., Sanchez-Vila, X. and Manzoni, S.: Ecological and soil hydraulic implications of microbial responses to stress - A modeling analysis, Adv. Water Resour., doi:10.1016/j.advwatres.2017.11.005, 2018.

Cable, J. M., Ogle, K., Williams, D. G., Weltzin, J. F. and Huxman, T. E.: Soil texture drives responses of soil respiration to precipitation pulses in the Sonoran Desert: Implications for climate change, Ecosystems, 11(6), 961–979, 2008.

Carbone, M. S., Still, C. J., Ambrose, A. R., Dawson, T. E., Williams, A. P., Boot, C. M., Schaeffer, S. M. and Schimel, J. P.: Seasonal and episodic moisture controls on plant and microbial contributions to soil respiration, Oecologia, 167(1), 265–278, 2011.

Cox, D. R. and Miller, H. D.: The theory of stochastic processes, Chapman & Hall/CRC., 2001.

Daly, E., Oishi, A. C., Porporato, A. and Katul, G. G.: A stochastic model for daily subsurface CO2 concentration and related soil respiration, Adv. Water Resour., 31(7), 987–994, 2008.

Daly, E., Palmroth, S., Stoy, P., Siqueira, M., Oishi, A. C., Juang, J. Y., Oren, R., Porporato, A. and Katul, G. G.: The effects of elevated atmospheric CO2 and nitrogen amendments on subsurface CO2 production and concentration dynamics in a maturing pine forest, Biogeochemistry, 94(3), 271–287, 2009.

Dijkstra, F. A., Augustine, D. J., Brewer, P. and von Fischer, J. C.: Nitrogen cycling and water pulses in semiarid grasslands: are microbial and plant processes temporally asynchronous?, Oecologia, 170(3), 799–808, doi:10.1007/s00442-012-2336-6, 2012.

Fierer, N. and Schimel, J. P.: Effects of drying-rewetting frequency on soil carbon and nitrogen transformations, Soil Biol. Biochem., 34(6), 777–787, 2002.

Fierer, N. and Schimel, J. P.: A proposed mechanism for the pulse in carbon dioxide production commonly observed following the rapid rewetting of a dry soil, Soil Sci. Soc. Am. J., 67(3), 798–805, 2003.

Fischer, T.: Substantial rewetting phenomena on soil respiration can be observed at low water availability, Soil Biol. Biochem., 41(7), 1577–1579, doi:10.1016/j.soilbio.2009.04.009, 2009.

Guo, X., Drury, C. F., Yang, X. and Reynolds, W. D.: Water-Soluble Carbon and the Carbon Dioxide Pulse are Regulated by the Extent of Soil Drying and Rewetting, Soil Sci. Soc. Am. J., 78(4), 1267–1278, doi:10.2136/sssaj2014.02.0059, 2014.

https://doi.org/10.5194/bg-2020-95
Preprint. Discussion started: 6 April 2020

Guo, Y. Y., Gong, P., Amundson, R. and Yu, Q.: Analysis of factors controlling soil carbon in the conterminous United States, Soil Sci. Soc. Am. J., 70(2), 601–612, 2006.

Harper, C. W., Blair, J. M., Fay, P. A., Knapp, A. K. and Carlisle, J. D.: Increased rainfall variability and reduced rainfall amount decreases soil CO2 flux in a grassland ecosystem, Glob. Change Biol., 11(2), 322–334, 2005.

Homyak, P. M., Blankinship, J. C., Slessarev, E., Schaeffer, S. M., Manzoni, S. and Schimel, J. P.: Effects of altered dry-season length and plant inputs on soluble soil carbon, Ecology, 99(10), 2348–2362, 2018.

Huxman, T. E., Smith, M. D., Fay, P. A., Knapp, A. K., Shaw, M. R., Loik, M. E., Smith, S. D., Tissue, D. T., Zak, J. C., Weltzin, J. F., Pockman, W. T., Sala, O. E., Haddad, B. M., Harte, J., Koch, G. W., Schwinning, S., Small, E. E. and Williams, D. G.: Convergence across biomes to a common rain-use efficiency, Nature, 429(6992), 651–654, doi:10.1038/nature02561, 2004.

IPCC: Managing the Risks of Extreme Events and Disasters to Advance Climate Change Adaptation (SREX). A Special Report of Working Groups I and II of the Intergovernmental Panel on Climate Change, edited by C. B. Field, V. Barros, T. F. Stocker, Q. D., Dokken D. J., K. L. Ebi, M. D. Mastrandrea, K. J. Mach, G.-K. Plattner, S. K. Allen, M. Tignor, and P. M. Midgley, , 582, 2012.

Jarvis, P., Rey, A., Petsikos, C., Wingate, L., Rayment, M., Pereira, J., Banza, J., David, J., Miglietta, F., Borghetti, M., Manca, G. and Valentini, R.: Drying and wetting of Mediterranean soils stimulates decomposition and carbon dioxide emission: the "Birch effect," Tree Physiol., 27(7), 929–940, 2007.

Katul, G., Porporato, A. and Oren, R.: Stochastic dynamics of plant-water interactions, Annu. Rev. Ecol. Evol. Syst., 38, 767–791, 2007.

Kim, D. G., Vargas, R., Bond-Lamberty, B. and Turetsky, M. R.: Effects of soil rewetting and thawing on soil gas fluxes: a review of current literature and suggestions for future research, Biogeosciences, 9(7), 2459–2483, doi:10.5194/bg-9-2459-2012, 2012.

Kottegoda, N. T. and Rosso, R.: Statistics, probability and reliability for civil and environmental engineers, McGraw-Hill, New York., 1998.

Lado-Monserrat, L., Lull, C., Bautista, I., Lidon, A. and Herrera, R.: Soil moisture increment as a controlling variable of the "Birch effect". Interactions with the pre-wetting soil moisture and litter addition, Plant Soil, 379(1–2), 21–34, doi:10.1007/s11104-014-2037-5, 2014.

Laio, F., Porporato, A., Ridolfi, L. and Rodriguez-Iturbe, I.: Plants in water-controlled ecosystems: active role in hydrologic processes and response to water stress - II. Probabilistic soil moisture dynamics, Adv. Water Resour., 24(7), 707–723, 2001.

Lawrence, C. R., Neff, J. C. and Schimel, J. P.: Does adding microbial mechanisms of decomposition improve soil organic matter models? A comparison of four models using data from a pulsed rewetting experiment, Soil Biol. Biochem., 41(9), 1923–1934, 2009.

Li, D. C., Velde, B. and Zhang, T. L.: Observations of pores and aggregates during aggregation in some clay-rich agricultural soils as seen in 2D image analysis, Geoderma, 118(3–4), 191–207, 2004.

Luyssaert, S., Inglima, I., Jung, M., Richardson, A. D., Reichstein, M., Papale, D., Piao, S. L., Schulzes, E. D., Wingate, L., Matteucci, G., Aragao, L., Aubinet, M., Beers, C., Bernhofer, C., Black, K. G., Bonal, D., Bonnefond, J. M., Chambers, J., Ciais, P., Cook, B., Davis, K. J., Dolman, A. J., Gielen, B., Goulden, M., Grace, J., Granier, A., Grelle, A., Griffis, T., Grunwald, T., Guidolotti, G., Hanson, P. J., Harding, R., Hollinger, D. Y., Hutyra, L. R., Kolar, P., Kruijt, B., Kutsch, W., Lagergren, F., Laurila, T., Law, B. E., Le Maire, G., Lindroth, A., Loustau, D., Malhi, Y., Mateus, J., Migliavacca, M., Misson, L., Montagnani, L., Moncrieff, J., Moors, E., Munger, J. W., Nikinmaa, E., Ollinger, S. V., Pita, G., Rebmann, C., Roupsard, O., Saigusa, N., Sanz, M. J., Seufert, G., Sierra, C., Smith, M. L., Tang, J., Valentini, R., Vesala, T. and Janssens, I. A.: CO2 balance of boreal, temperate, and tropical forests derived from a global database, Glob. Change Biol., 13(12), 2509–2537, doi:10.1111/j.1365-2486.2007.01439.x, 2007.

https://doi.org/10.5194/bg-2020-95
Preprint. Discussion started: 6 April 2020

Manzoni, S. and Katul, G.: Invariant soil water potential at zero microbial respiration explained by hydrological discontinuity in dry soils, Geophys. Res. Lett., 41(20), 2014GL061467, doi:10.1002/2014GL061467, 2014.

Manzoni, S., Schimel, J. P. and Porporato, A.: Responses of soil microbial communities to water stress: results from a meta-analysis, Ecology, 93(4), 930–938, 2012.

Manzoni, S., Moyano, F., Kätterer, T. and Schimel, J.: Modeling coupled enzymatic and solute transport controls on decomposition in drying soils, Soil Biol. Biochem., 95, 275–287, doi:10.1016/j.soilbio.2016.01.006, 2016.

Messori, G., Ruiz-Pérez, G., Manzoni, S. and Vico, G.: Climate drivers of the terrestrial carbon cycle variability in Europe, Environ. Res. Lett., 14(6), 063001, doi:10.1088/1748-9326/ab1ac0, 2019.

Miller, A. E., Schimel, J. P., Meixner, T., Sickman, J. O. and Melack, J. M.: Episodic rewetting enhances carbon and nitrogen release from chaparral soils, Soil Biol. Biochem., 37(12), 2195–2204, 2005.

Moyano, F. E., Vasilyeva, N., Bouckaert, L., Cook, F., Craine, J., Yuste, J. C., Don, A., Epron, D., Formanek, P., Franzluebbers, A., Ilstedt, U., Katterer, T., Orchard, V., Reichstein, M., Rey, A., Ruamps, L., Subke, J. A., Thomsen, I. K. and Chenu, C.: The moisture response of soil heterotrophic respiration: interaction with soil properties, Biogeosciences, 9(3), 1173–1182, doi:10.5194/bg-9-1173-2012, 2012.

Moyano, F. E., Manzoni, S. and Chenu, C.: Responses of soil heterotrophic respiration to moisture availability: An exploration of processes and models, Soil Biol. Biochem., 59(0), 72–85, doi:10.1016/j.soilbio.2013.01.002, 2013.

Porporato, A., Daly, E. and Rodriguez-Iturbe, I.: Soil water balance and ecosystem response to climate change, Am. Nat., 164(5), 625–632, 2004.

Reichstein, M., Bahn, M., Ciais, P., Frank, D., Mahecha, M. D., Seneviratne, S. I., Zscheischler, J., Beer, C., Buchmann, N., Frank, D. C., Papale, D., Rammig, A., Smith, P., Thonicke, K., van der Velde, M., Vicca, S., Walz, A. and Wattenbach, M.: Climate extremes and the carbon cycle, Nature, 500(7462), 287–295, doi:10.1038/nature12350, 2013.

Ridolfi, L., D'Odorico, P., Porporato, A. and Rodriguez-Iturbe, I.: The influence of stochastic soil moisture dynamics on gaseous emissions of NO, N2O, and N-2, Hydrol. Sci. J.-J. Sci. Hydrol., 48(5), 781–798, 2003.

Rodriguez-Iturbe, I. and Porporato, A.: Ecohydrology of Water-Controlled Ecosystems. Soil Moisture and Plant Dynamics, Cambridge University Press, Cambridge., 2004.

Rubio, V. E. and Detto, M.: Spatiotemporal variability of soil respiration in a seasonal tropical forest, Ecol. Evol., 7(17), 7104–7116, doi:10.1002/ece3.3267, 2017.

Schaeffer, S. M., Homyak, P. M., Boot, C. M., Roux-Michollet, D. and Schimel, J. P.: Soil carbon and nitrogen dynamics throughout the summer drought in a California annual grassland, Soil Biol. Biochem., 115, 54–62, doi:10.1016/j.soilbio.2017.08.009, 2017.

Schimel, J. P., Balser, T. C. and Wallenstein, M.: Microbial stress-response physiology and its implications for ecosystem function, Ecology, 88(6), 1386–1394, 2007.

Shi, A. and Marschner, P.: The number of moist days determines respiration in drying and rewetting cycles, Biol. Fertil. Soils, 51(1), 33–41, doi:10.1007/s00374-014-0947-2, 2015.

Shi, A. D. and Marschner, P.: Drying and rewetting frequency influences cumulative respiration and its distribution over time in two soils with contrasting management, Soil Biol. Biochem., 72, 172–179, doi:10.1016/j.soilbio.2014.02.001, 2014.

Sierra, C. A., Harmon, M. E., Thomann, E., Perakis, S. S. and Loescher, H. W.: Amplification and dampening of soil respiration by changes in temperature variability, Biogeosciences, 8(4), 951–961, doi:10.5194/bg-8-951-2011, 2011.

Slessarev, E. W. and Schimel, J. P.: Partitioning sources of CO2 emission after soil wetting using high-resolution observations and minimal models, Soil Biol. Biochem., 143, 107753, doi:10.1016/j.soilbio.2020.107753, 2020.

Unger, S., Maguas, C., Pereira, J. S., David, T. S. and Werner, C.: The influence of precipitation pulses on soil respiration - Assessing the "Birch effect" by stable carbon isotopes, Soil Biol. Biochem., 42(10), 1800–1810, doi:10.1016/j.soilbio.2010.06.019, 2010.

https://doi.org/10.5194/bg-2020-95
Preprint. Discussion started: 6 April 2020

Williams, M. A. and Xia, K.: Characterization of the water soluble soil organic pool following the rewetting of dry soil in a drought-prone tallgrass prairie, Soil Biol. Biochem., 41(1), 21–28, doi:10.1016/j.soilbio.2008.08.013, 2009.

Xiang, S. R., Doyle, A., Holden, P. A. and Schimel, J. P.: Drying and rewetting effects on C and N mineralization and microbial activity in surface and subsurface California grassland soils, Soil Biol. Biochem., 40(9), 2281–2289, 2008.

Yan, L., Chen, S., Xia, J. and Luo, Y.: Precipitation Regime Shift Enhanced the Rain Pulse Effect on Soil Respiration in a Semi-Arid Steppe, PLOS ONE, 9(8), e104217, doi:10.1371/journal.pone.0104217, 2014.

Zhang, B., Tan, X., Wang, S., Chen, M., Chen, S., Ren, T., Xia, J., Bai, Y., Huang, J. and Han, X.: Data from: Asymmetric sensitivity of ecosystem carbon and water processes in response to precipitation change in a semi-arid steppe, Dryad Digit. Repos., doi:https://doi.org/10.5061/dryad.vf8d2, 2017a.

Zhang, B. W., Tan, X. R., Wang, S. S., Chen, M. L., Chen, S. P., Ren, T. T., Xia, J. T., Bai, Y. F., Huang, J. H. and Han, X. G.: Asymmetric sensitivity of ecosystem carbon and water processes in response to precipitation change in a semi-arid steppe, Funct. Ecol., 31(6), 1301–1311, doi:10.1111/1365-2435.12836, 2017b.

Zhang, B. W., Li, W. J., Chen, S. P., Tan, X. R., Wang, S. S., Chen, M. L., Ren, T. T., Xia, J. Y., Huang, J. H. and Han, X. G.: Changing precipitation exerts greater influence on soil heterotrophic than autotrophic respiration in a semiarid steppe, Agric. For. Meteorol., 271, 413–421, doi:10.1016/j.agrformet.2019.03.019, 2019.

Zhang, B. W., Cadotte, M. W., Chen, S. P., Tan, X. R., You, C. H., Ren, T. T., Chen, M. L., Wang, S. S., Li, W. J., Chu, C. J., Jiang, L., Bai, Y. F., Huang, J. H. and Han, X. G.: Plants alter their vertical root distribution rather than biomass allocation in response to changing precipitation, Ecology, doi:10.1002/ecy.2828, 2020.

Zhang, Q., Phillips, R. P., Manzoni, S., Scott, R. L., Oishi, A. C., Finzi, A., Daly, E., Vargas, R. and Novick, K. A.: Changes in photosynthesis and soil moisture drive the seasonal soil respiration-temperature hysteresis relationship, Agric. For. Meteorol., 259, 184–195, doi:10.1016/j.agrformet.2018.05.005, 2018.

https://doi.org/10.5194/bg-2020-95
Preprint. Discussion started: 6 April 2020

565 **Table 1: Symbol definitions and units. Symbol p_z represents the probability density function (PDF) of the stochastic variable z indicated in the subscript.**

Symbol	Definition	Units
b	Parameter in the rewetting respiration equation	-
C	Normalization constant in the soil moisture PDF	-
C'	Parameter group, $C' = \left(\Gamma\left[\frac{\lambda}{\eta}\right] - \Gamma\left[\frac{\lambda}{\eta}, \gamma\right]\right)^{-1}$	-
E	Evapotranspiration rate	m d^{-1}
E_{max}	Evapotranspiration rate at the soil field capacity	m d^{-1}
h	Precipitation event depth	m
L	Rate of water loss via deep percolation and surface runoff	m d^{-1}
J	Jacobian matrix	
n	Soil porosity	-
$p_{R_d}(R_d)$	PDF of the soil respiration rate during dry-down periods	gC^{-1} m^2 d
$p_{R_r}(R_r)$	PDF of the respired carbon at rewetting	gC^{-1} m^2
$p_x(x)$	PDF of normalized soil moisture (x)	-
$p_{x_d}(x_d)$	PDF of normalized soil moisture at the end of the dry period (x_d)	-
$p_{X,R_r}(X, R_r)$	Joint PDF of the auxiliary variable X and of the respired carbon at rewetting (R_r)	gC^{-1} m^2 d
$p_y(y)$	Marginal PDF of soil moisture increase due to precipitation (y)	-
$p_y(y\|x_d)$	PDF of soil moisture increase due to precipitation (y) conditional on soil moisture at the end of the previous dry period (x_d)	-
$p_{y,x_d}(y, x_d)$	Joint PDF of soil moisture at the end of a dry period (x_d) and soil moisture increase due to precipitation (y)	-
P	Precipitation rate	m d^{-1}
r_d	Normalized respiration rate during drying, $r_d = R_d/R_{d,max}$	-
r_r	Normalized respired carbon at rewetting, $r_r = R_r/R_{r,max}$	-
R_d	Respiration rate during dry-down periods	gC m^{-2} d^{-1}
$R_{d,max}$	Maximum respiration rate at the soil field capacity	gC m^{-2} d^{-1}
R_r	Respired carbon at rewetting	gC m^{-2}
$R_{r,max}$	Maximum respired carbon at rewetting (for y=1, x_d=0)	gC m^{-2}
$\langle R_r^* \rangle$	Mean rate of respiration from rewetting pulses	gC m^{-2} d^{-1}
$\langle R_t \rangle$	Mean total respiration rate (sum of $\langle R_d \rangle$ and $\langle R_r^* \rangle$)	gC m^{-2} d^{-1}
s	Relative volumetric soil moisture (i.e., saturation)	-
s_w, s_1	Soil moisture at the wilting point and at field capacity, respectively	-
t	Time	d
x	Normalized soil moisture, $x = \frac{s - s_w}{s_1 - s_w}$	-
x_d	Normalized soil moisture at the end of a dry period	-
X	Auxiliary variable, X=x_d	-
y	Change in normalized soil moisture at rewetting	-
Z_r	Soil rooting depth	m
α	Mean precipitation event depth	m

https://doi.org/10.5194/bg-2020-95
Preprint. Discussion started: 6 April 2020

γ	Parameter group, $\gamma = \frac{nZ_r(s_1 - s_w)}{\alpha}$	-
$\Gamma[\cdot]$	Gamma function, $\Gamma[z] = \int_0^\infty u^{z-1}e^{-u}du$	-
$\Gamma[\cdot,\cdot]$	Incomplete gamma function, $\Gamma[a,z] = \int_z^\infty u^{a-1}e^{-u}du$	-
$\delta[\cdot]$	Dirac delta function	[argument]$^{-1}$
η	Parameter group, $\eta = \frac{E_{max}}{nZ_r(s_1 - s_w)}$	-
λ	Mean frequency of precipitation events	d^{-1}
σ_{R_d}	Standard deviation of the respiration rate during drying	gC m^{-2} d^{-1}
σ_{R_r}	Standard deviation of the respiration pulse at rewetting	gC m^{-2}
$\theta[\cdot]$	Heaviside step function	-
$\langle\cdot\rangle$	Long term average	[argument]

https://doi.org/10.5194/bg-2020-95
Preprint. Discussion started: 6 April 2020

570 **Table 2: Characteristics of the selected mineral (top three) and organic soil samples (bottom three), and parameter estimates and coefficients of determination (R^2) for the least square fit of Eq. (13) (see also Figure 2).**

Soil	Organic C (g/kg)	Bulk density (g/cm^3)	$R_{d,max}$ (gC m^{-2} d^{-1})	$R_{r,max}$ (gC m^{-2})	b (-)	R^2	Source
Chelva sandy loam	10.9	1.44	0.79	0.89	0.17	0.74	(Lado-Monserrat et al., 2014)
Tuéjar clay loam	26.6	1.19	0.13	0.25	0.14	0.92	(Lado-Monserrat et al., 2014)
Brookston clay loam	28.6	1.24	1.49	8.79	0.04	0.76	(Guo et al., 2014)
Neuglobsow sand	440	0.14	1.05	13.95	0.10	0.87	(Fischer, 2009)
Taura silty sand	390	0.15	1.26	11.23	0.10	0.86	(Fischer, 2009)
Rösa sand	340	0.18	1.53	18.61	0.12	0.83	(Fischer, 2009)

https://doi.org/10.5194/bg-2020-95
Preprint. Discussion started: 6 April 2020

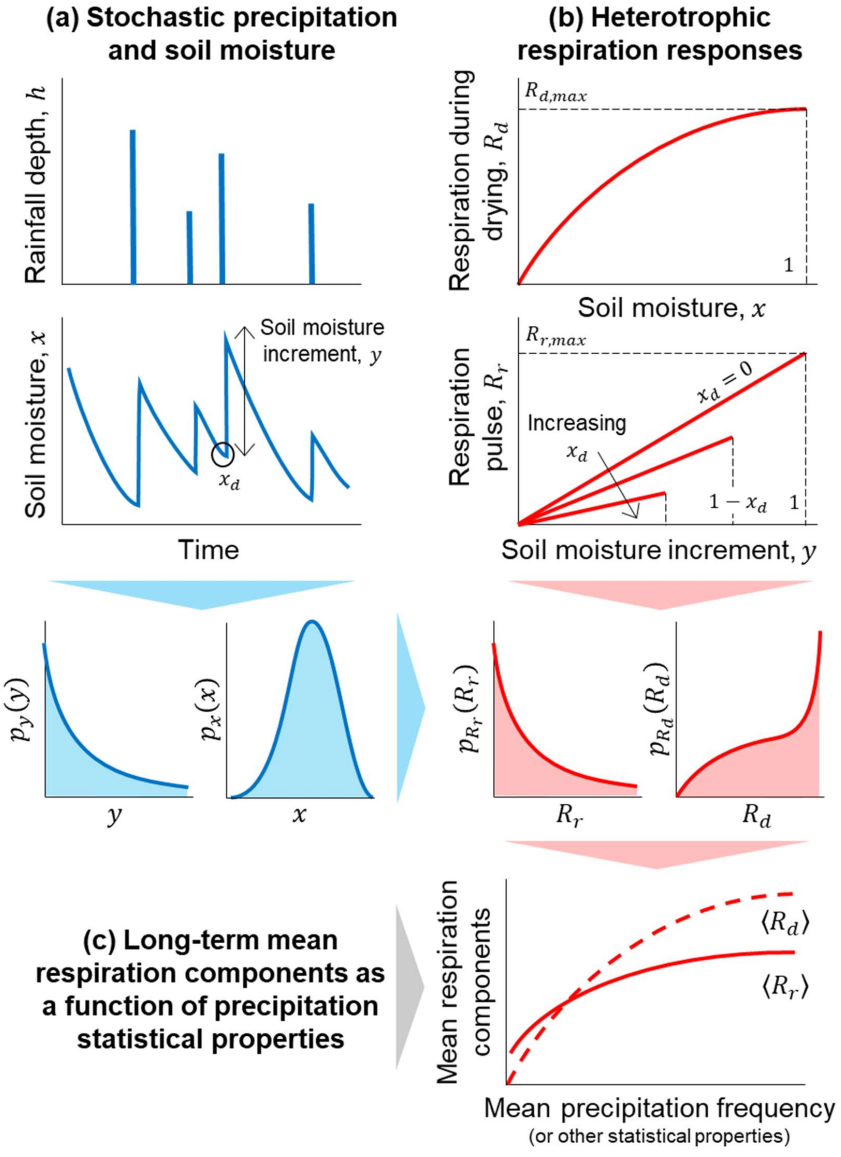

Figure 1: Schematic illustration of the theoretical framework developed to describe how the components of heterotrophic respiration change as a function of rainfall statistical properties. (a) Rainfall is treated as a stochastic process driving random fluctuations in soil moisture, which are captured by the probability density functions (PDF, indicated by *p* with a subscript for the variable of interest) of soil moisture (*x*) and soil moisture increments (*y*). (b) Respiration rate during drying (R_d) and respiration pulses at rewetting (R_r) respectively depend on soil moisture, and on both soil moisture increments and soil moisture at the end of the dry period (x_d); based on the PDF of *x*, *y*, and x_d, the PDF of the two respiration components are obtained. (c) Using these PDF of respiration, long term mean respiration rate during drying ($<R_d>$) and respiration pulses ($<R_r>$) are calculated and their relations with the statistical properties of precipitation are analysed.

https://doi.org/10.5194/bg-2020-95
Preprint. Discussion started: 6 April 2020

585

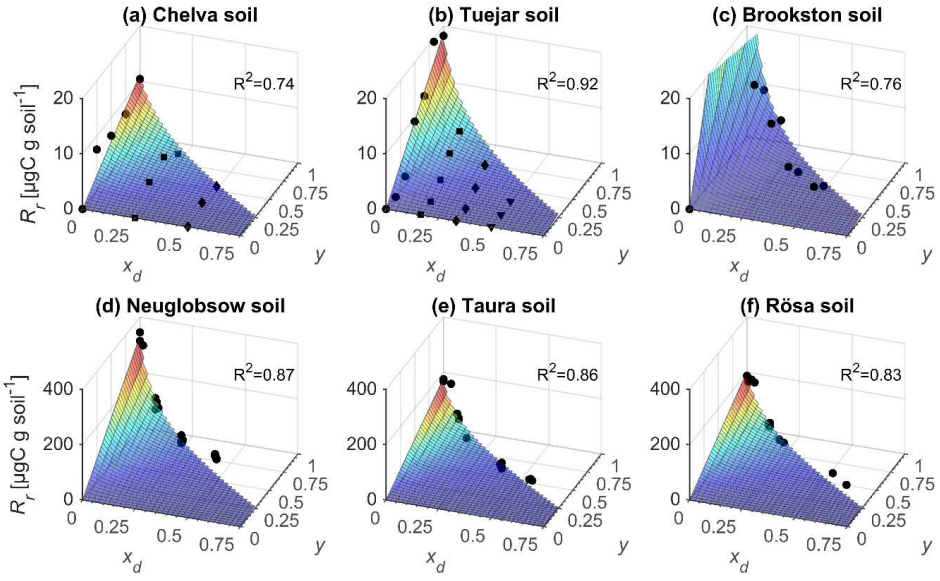

Figure 2: Relations between respiration pulse size (R_r) and pre-wetting soil moisture (x_d) and soil moisture increment at rewetting (y), for six soils; top row: mineral soils; bottom row: organic soils (note different vertical scales between rows). Symbols represent measured respiration pulses and surfaces are fitted R_r functions from Eq. (13) (soil characteristics, fitting parameters, and data sources are reported in Table 2).

590

https://doi.org/10.5194/bg-2020-95
Preprint. Discussion started: 6 April 2020

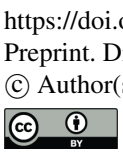

Biogeosciences
Discussions
Open Access
EGU

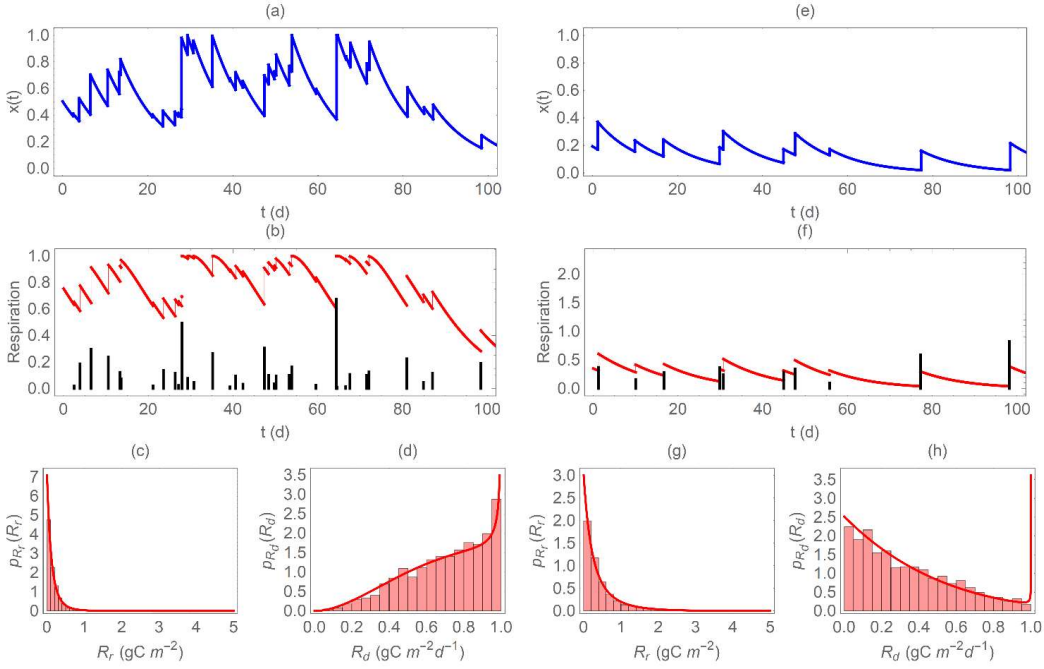

Figure 3: Example of the dynamics of soil moisture and respiration for a wet (a-d) and a dry climate (e-h). Top panels (a, e) show the simulated trajectories of normalized soil moisture *x*; the middle panels (b, f) show the trajectories of respiration during dry periods (red solid curves, R_d) and the respiration pulse at rewetting (black vertical bars, R_r, on the same scale despite different units); the bottom panels (c, d, g, h) show the probability density functions of R_r and R_d ($p_{R_r}(R_r)$ and $p_{R_d}(R_d)$, respectively) overlapped to the histograms of the simulated data. In this figure, $R_{r,max}$=5 gC m^{-2}, $R_{d,max}$=1 gC m^{-2} d^{-1}, b=0.1, γ =5, η =0.1 d^{-1}, and λ =0.3 and 0.1 d^{-1} (panels a-d and e-h, respectively).

https://doi.org/10.5194/bg-2020-95
Preprint. Discussion started: 6 April 2020

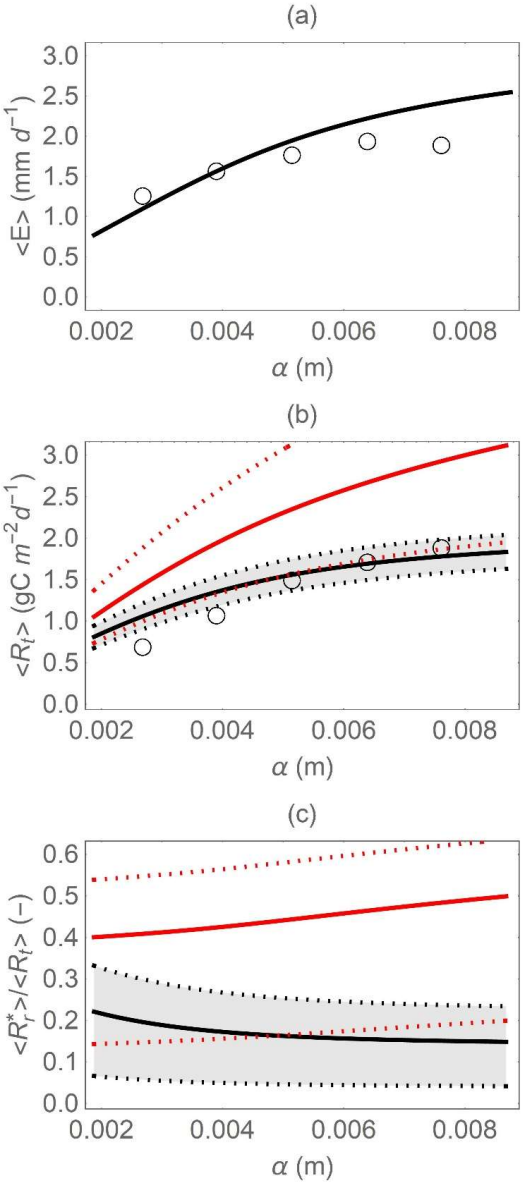

600

Figure 4: Comparison of model results (curves) and observations (open circles) along an experimental rainfall gradient where the mean precipitation depth (α) was manipulated: (a) mean evapotranspiration rate, (b) mean total heterotrophic respiration rate, and (c) fraction of the total heterotrophic respiration rate due to rewetting pulses . In panels (b) and (c), the dotted curves and shaded area indicate the variation caused by changes in $R_{r,max}$ between 5 and 35 g m^{-2} around the central value (solid curves) of 25 g m^{-2}; the red curves indicate results using the simplified rewetting respiration model (Eq. (21)). Parameter values are described in Section 2.2.2.

605

https://doi.org/10.5194/bg-2020-95
Preprint. Discussion started: 6 April 2020

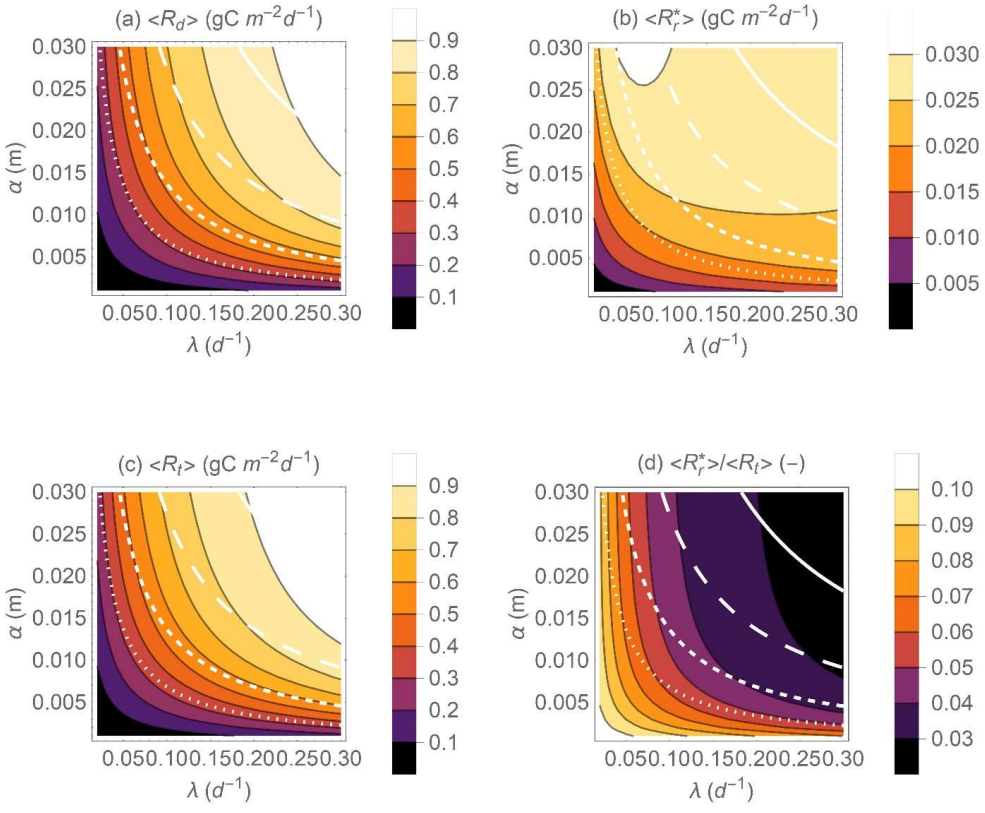

Figure 5: Effect of precipitation statistical properties (mean event frequency λ and depth α) on the mean heterotrophic respiration rates during dry periods $\langle R_d \rangle$ (a), and at rewetting $\langle R_r^* \rangle$ (b), the mean total respiration rate $\langle R_t \rangle$ (c), and on the fraction of the total heterotrophic respiration rate due to rewetting pulses $\langle R_r^* \rangle / \langle R_t \rangle$ (d). The white contour curves indicate combinations of λ and α that generate different annual precipitation rates ($\langle P \rangle = \alpha\lambda$ =0.25, 0.5, 1, and 2 m y^{-1} from dotted to solid lines). Other parameter values: $R_{r,max}$=5 gC m^{-2}, $R_{d,max}$=1 gC m^{-2} d^{-1}, b=0.1, Z_r=0.3 m, n=0.5, s_w=0.2, s_1=0.7, E_{max}=0.0037 m d^{-1}.

https://doi.org/10.5194/bg-2020-95
Preprint. Discussion started: 6 April 2020

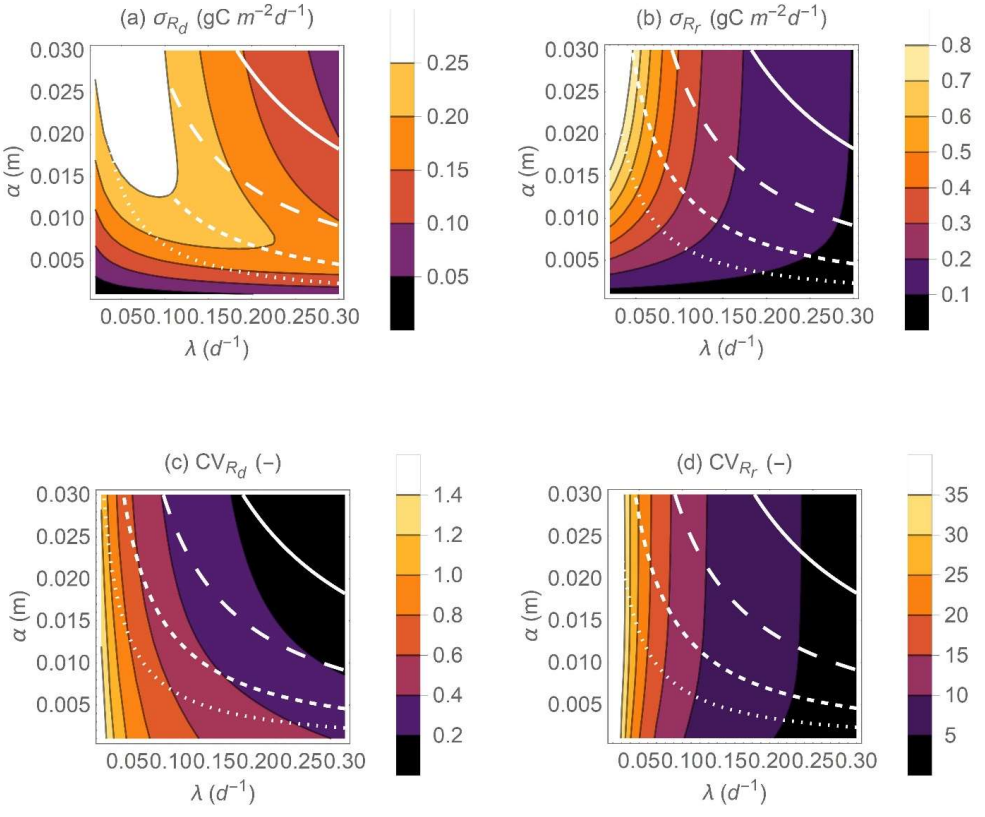

615

Figure 6: Effect of precipitation statistical properties (mean event frequency λ and depth α) on the standard deviations of heterotrophic respiration rates during dry periods σ_{R_d} (a) and respiration pulses at rewetting σ_{R_r} (b), and on the coefficients of variations of respiration rates during dry periods CV_{R_d} (c) and respiration pulses at rewetting CV_{R_r} (d). The white contour curves indicate combinations of λ and α that generate different annual precipitation rates ($\langle P \rangle = \alpha\lambda$ =0.25, 0.5, 1, and 2 m y^{-1} from dotted to solid lines). Other parameter values are as in Figure 5.

620